Astron. Astrophys. 343, 939–942 (1999)

ASTRONOMY AND ASTROPHYSICS

A search for methanol masers at 9.978 GHz and 10.058 GHz

M. Röllig[1], **W.H. Kegel**[1], **R. Mauersberger**[2], **and C. Doerr**[1]

[1] Institut für theoretische Physik, Universität Frankfurt, Robert-Mayer-Strasse 10, D-60054 Frankfurt am Main, Germany (roellig@astro.uni-frankfurt.de)
[2] Steward Observatory, The University of Arizona, Tucson, AZ 85721, USA (mauers@as.arizona.edu)

Received 26 October 1998 / Accepted 8 December 1998

Abstract. We performed NLTE-radiative transfer calculations for interstellar A-type methanol maser lines in order to find out under which physical conditions the level populations show strong inversion. In our model we considered collisional as well as radiative pumping and accounted for line overlap as well as for torsional excitation of the methanol molecules. The radiation field was calculated using a simple on-the-spot approximation. Our results show that torsional excitation can be essential for the maser pumping mechanism while line overlap appears to be of minor importance. In addition to the well known Class I and Class II maser lines, we found two new transitions which possibly may show up as strong masers. These are the 4_3–5_2 A^- and A^+ transitions at $10.058\,\mathrm{GHz}$ and $9.978\,\mathrm{GHz}$ respectively. These masers are radiatively pumped by IR radiation, i.e. they should be found near IR sources similar to the classical Class II methanol masers. 88 galactic CH_3OH maser sources were searched for emission in these two lines, but no detection was made. Upper limits are given and discussed.

Key words: radio lines: ISM – ISM: H II regions – ISM: molecules – radiative transfer – masers

1. Introduction

Maser transitions of A and E-type methanol belong to the strongest molecular lines observed in the Galaxy. They are related to star forming regions. Following the convention introduced by Menten (1991), the two existing types of methanol maser lines are labeled Class I and Class II. Class II masers are found near compact H II regions while Class I masers are offset from IR sources and are not associated with compact H II regions (Cragg et al., 1992). The excitation of Class I methanol masers is relatively well understood and arises due to collisional pumping (Cragg et al., 1992). On the other hand the pumping mechanism of Class II masers is not fully understood yet, but they are believed to be radiatively pumped. In order to get deeper insight into the pumping mechanism of A-type methanol maser lines, we performed extensive radiative transfer calculations based on a simple on-the-spot approximation, which enabled us to vary the physical parameters over a wide range. While this approximation is very crude, it appears well suited to study the *relative* importance of different physical effects. During the course of this investigation we found two new transitions for which population inversions are predicted and which possibly may show strong maser emission. Motivated by these results, we searched for these lines in 88 sources of 6.6 GHz maser radiation.

Send offprint requests to: M. Röllig (roellig@astro.uni-frankfurt.de)

2. Numerical results

The physical model and the mathematical aproximations underlying our computations, are briefly described in the Appendix. The results may be summerized as follows.

Contrary to our initial expectation, accounting for line overlap introduces only minor changes in the results. On the other hand we found that the inclusion of the levels of the first torsionally excited state may change the results qualitatively. This is in particular true if one accounts for an IR background. But at higher kinetic temperatures ($T \approx 100\,\mathrm{K}$) the torsionally excited levels become important even without IR background.

In general our findings are consistent with previous results of other authors. In particular we confirm that the Class I masers are collisionally pumped (see e.g. Cragg et al. 1992). The inversion is increasing with increasing kinetic temperature. A background radiation field has the tendency to reduce the inversion. Similar to the results of Sobolev et al. (1997), our results show that type II masers and in particular the $5_1 - 6_0\mathrm{A}^+$ transition, can be effectively pumped by the IR radiation of warm dust. With $T_{\mathrm{dust}} = 80$ K we found optical depths as low as -8 (Fig. 2) and brightness temperatures of the order 10^4K. We made no attempt to adjust our free parameters in order to simulate observed data. The results of Sobolev et al. (1997) indicate that the dust temperature in the observed maser regions may be considerably higher (> 150 K). - Furthermore our results indicate that in principle type II masers may also be collisionally pumped if the kinetic temperature is sufficiently high (≥ 100 K).

In addition we found two new transitions which according to our numerical results should show inversion of the occupation numbers in a wide range of parameters and possibly may show up as fairly strong masers. These are the transitions $4_3 - 5_2$ A^- and A^+ at $10.058\,\mathrm{GHz}$ and $9.978\,\mathrm{GHz}$, respectively. The conditions under which we find inversion for these lines are similar to those found for the $5_1 - 6_0\mathrm{A}^+$ transition, i.e. these lines are very effectively pumped by the IR radiation of warm dust. Also the maximal brightness temperature is comparable, though some-

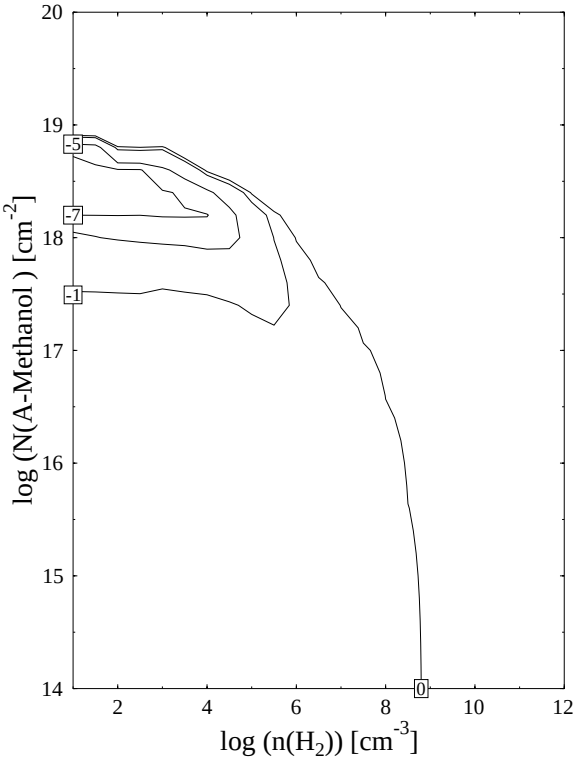

Fig. 1. (log $N_{\rm CH_3OH}$ - log $n_{\rm H_2}$)-diagram with iso-τ lines for the $4_3 - 5_2$ A$^-$ transition. Results refer to $T_{\rm kin} = 20\,{\rm K}$ and $T_{\rm dust} = 80\,{\rm K}$. $N_{\rm CH_3OH}$ is normalized to $^{\Delta\nu}/_{\nu_0} = 10^{-5}$. The τ-values are $0, -1, -5,$ and -7.

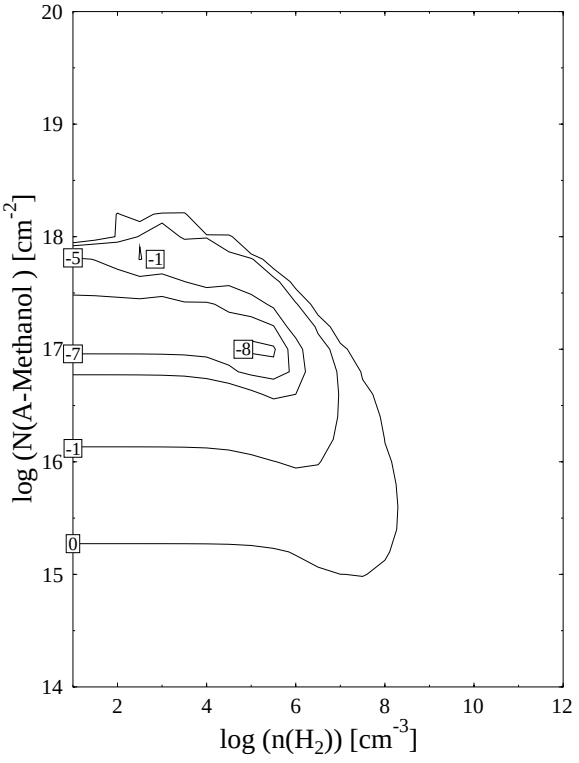

Fig. 2. Same as Fig. 1 but for the $5_1 - 6_0$ A$^+$ transition. The innermost contour corresponds to $\tau = -8$.

what lower, to that of the $5_1 - 6_0$A$^+$ maser. Furthermore we found weaker inversions under similar conditions for the two transitions $3_3 - 4_2$ A$^-$ and A$^+$ at $5.842\,$GHz and $5.839\,$GHz, respectively.

Fig. 1 gives the numerical results we obtained for the $4_3 - 5_2$ A$^-$ transition with $T_{\rm kin} = 20\,{\rm K}$ and $T_{\rm dust} = 80\,{\rm K}$. Shown are lines of equal optical depth in a (log $N_{\rm CH_3OH}$-log $n_{\rm H_2}$)-diagram, where $N_{\rm CH_3OH}$ is normalized to a relative line width $^{\Delta\nu}/_{\nu_0}$ of 10^{-5}. For comparison Fig. 2 shows the corresponding diagram for the $5_1 - 6_0$ A$^+$ transition. We see that the regions of inversion are similar in general, however, the regions of maximal inversion for the $4_3 - 5_2$ A$^-$ transition is shifted to higher column densities and lower H_2 densities as compared to the $5_1 - 6_0$ A$^+$ transition. The results for the $4_3 - 5_2$ A$^+$ transition are very similar to those for the corresponding A$^-$ transition.

Our results also indicate for the new maser lines as well as for the $5_1 - 6_0$ A$^+$ transition and other type II maser lines that at high kinetic temperature ($T_{\rm kin} \geq 100$ K) inversion may also be achieved by collisional pumping.

According to the similarity in the pumping mechanism, these newly predicted masers belong to the Class II masers.

3. Observations

All observations were conducted May 24-26 1998 with the 140 ft. radiotelescope of the National Radioastronomy Observatory (NRAO[1]) in Greenbank.

The receiver was a dual polarization HFET installed in the Cassegrain focus. Only one polarization channel was used in order to allow a higher spectral bandwidth. A 1024 channel autocorrelation spectrometer was split into two halves, each with a bandwidth of 5 MHz (150 km s^{-1}) and a spectral resolution of 9.8 kHz (0.30 km s^{-1}), which were centered at the frequencies of the maser candidates, 9.9786 GHz and 10.0583 GHz (Lovas et al., 1984, priv. comm.). At those frequencies, the beam width is $3\farcm5$. We employed position switching, the reference position being at -6 minutes in R.A. and for each source we integrated 6 minutes on the reference and the same amount on the source. For some sources, this procedure was repeated one or several times to increase the signal-to-noise ratio. The flux density scale was established by continuum cross scans through NGC 7027, which has a flux density of 6.1 Jy in the X-band (Ott et al., 1994). The pointing was checked frequently on continuum sources. Typical pointing uncertainties are $< 10''$.The weather was cloudy with intermittent light rain. This should effect mostly the system temperature and calibration uncertainty of some sources with declinations as far south as $-40^{\rm o}$.

4. Observational results and discussion

We measured all 88 sources which were detected to be masers in the CH$_3$OH $5_1 - 6_0 A^+$ transition by Menten (1991), where also the coordinates are listed. Prominent sources in that list are, e.g. W3(OH), NGC 6334F, W75N or Cep A, along with many

[1] The NRAO is operated by Associated Universities, Inc. under contract with the National Science Foundation.

Table 1. Rms noise reached for the individual sources.

RMS (T_A^*)[a] mK	Sources[b]
15...25	W3(OH), W49N, W51, Cep A, NGC7538
25...35	S231, Sgr B2, 28.21-0.05, W43M
35...45	173.59+02.44, S252A, S252, S255, S269, NGC 2264, RCW 122, 354.61+0.48, 353.41-0.36, 355.34+0.15 359.14+0.03, 359.43-0.10, Sgr A-F, 359.62-0.25, Sgr A-A, 0.54-0.85, 2.14+0.01, 3.91-0.01, 9.62+0.19 8.67-0.37, W31(1), 10.62-0.38, 12.89+0.49, 11.91-0.15, 12.22-0.12, W33B, 11.94-0.62, W33, W33A, M17 16.59-0.06, 18.46-0.01, 19.48+0.16, 20.24+0.08, 20.08-0.13, 21.88+0.02, 22.44-0.18, 23.43-0.19 23.01-0.41, W42, 30.70-0.06, 30.79-0.06, 30.82-0.06, 32.74-0.07, 33.13-0.09, 34.26+0.15, 35.03+0.35 35.19-0.74, 35.20-0.73, 40.62-0.14, 43.80-0.13, 45.07+0.13, 45.47+0.13, 45.47+0.05, ON1, W75N DR21(OH), W75S(3)
45...55	345.01+1.79, 344.58-0.02, 345.51+0.35, 345.00-0.22, 345.70-0.09, 350.11+0.09, NGC6334B, NGC6334C NGC6334F, 351.78-0.54, 12.03-0.04, 24.33+0.11, 27.35-0.20, 29.95-0.02, 30.82+0.28, V645Cyg, ON2
55...65	Mon R2, 28.83-0.25, 30.22-0.15, 30.60-0.06

[a] in a 0.39 km s^{-1} wide velocity channel; multiply by a factor of 5 to obtain mJy/beam
[b] for coordinates, see Menten (1991)

compact H II regions and sources toward the Galactic Center region. In Table 1 we give for each source the approximate rms noise in mK antenna temperature (multiply by 5 to obtain mJy).

For most of the sources, the rms noise at a velocity resolution of 0.30 km s^{-1} was of order 200 mJy. No strong features have been detected. Our measurements exclude masers stronger than about 1 Jy.

These findings indicate that in the vicinity (i.e. within one beamwidth) of the 6.6 GHz masers reported by Menten (1991) the lines at 9.98 GHz and 10.06 GHz are not strongly inverted. On the other side, from our model calculations we would expect that whenever the occupation numbers of the $5_1 - 6_0$ A$^+$ transition are inverted, this is also true for the $4_3 - 5_2$ A$^-$ and A$^+$ transitions. Due to the crude approximations underlying our calculations it is difficult to make quantitative estimates of the intensities. If we, nevertheless, take our numerical results at face value and assume in addition that the physical conditions within the regions from which the 6.6 GHz radiation is emitted, correspond to the parameters for which we find the largest intensity for the 6.6 GHz line, we would expect for the lines at at 9.98 GHz and 10.06 GHz a brightness temperature of a few K. The expected flux, of course, depends on the source size. If the latter is about 0.″5 or less, our numerical results would still be consistent with our observational results. In this context it is of interest to note that Slysh et al. (1993) reported a marginal detection of the $5_1 - 6_0$ A$^-$ line in SgrB2 at a level of 0.04 Jy and a probable detection of the $5_1 - 6_0$ A$^+$ line in W33 at a level of 0.17 Jy.

Acknowledgements. It is a pleasure to thank Dr. Dana Balser for his valable support with the preparation of the observations. We also thank Dr. B. Deiss for stimulating discussions. Furthermore we are grateful to the authors of Moruzzi et al. (1995) for making their results available to us prior to publication. R.M. is supported by a Heisenberg fellowship by the Deutsche Forschungsgemeinschaft.

Appendix A: the physical model

A.1. Radiative transfer

The physical model and the general concept of the numerical methods have been discussed previously in some detail (Piehler and Kegel, 1989; Chandra et al., 1984; Kegel, 1979). The essential points are the following: In order to solve the coupled set of rate equations and the radiative transfer equations for all relevant lines, we consider a homogeneous model. In addition, in solving the rate equations we used only a spatial average of the quantity

$$\tilde{J}_{ik} = \frac{1}{4\pi} \int \int I_{ik}(\Delta\nu)\, \Phi(\Delta\nu)\, d\Omega d\Delta\nu \qquad \text{(A1)}$$

Here I_{ik} is the intensity in the line corresponding to the transition $k \rightarrow i$, and Φ is the profile function of the absorption coefficient. By this crude approximation the density of the molecules in any energy level also becomes homogeneous and the radiative transfer equation may be integrated analytically. Assuming further a rectangular line profile with a width $\Delta\nu$ corresponding to a velocity dispersion $\Delta v = c \cdot ({}^{\nu}/_{\nu_0})$, we finally obtain

$$\tilde{J}_{ik} = \tilde{S}_{ik} \left(1 - e^{-\tau_\nu}\right) + I_{bg} e^{-\tau_\nu} \qquad \text{(A2)}$$

where $\tilde{S}_{ik}$ is the effective source function (see below), τ_ν the optical depth in the line, and I_{bg} the background radiation eventually pumping the maser molecules.

The methanol molecule has a complex energy level diagram and a very large number of radiative transitions. Several pairs and triples of lines have almost identical frequencies, i.e. these lines overlap. It was one of the aims of the present study to investigate the importance of such line overlap for the pump process. We considered lines with frequency differences corresponding to $\Delta v \leq 0.1\,\mathrm{km/sec}$ as completely overlapping. In this case

we have for the effective source function $\tilde{S}_{ik}$ in the case of line pairs

$$\tilde{S}_\nu = S_1 + \frac{\kappa_2 \cdot (S_2 - S_1)}{\kappa_\nu} \tag{A3}$$

and in the case of triples

$$\tilde{S}_\nu = S_1 + \frac{\kappa_2 \cdot (S_2 - S_1)}{\kappa_\nu} + \frac{\kappa_3 \cdot (S_3 - S_1)}{\kappa_\nu} \tag{A4}$$

where κ_ν is the total absorption coefficient

$$\kappa_\nu = \sum \kappa_i \qquad i = 1, 2, 3 \tag{A5}$$

For single lines $\tilde{S}_{ik}$ is the usual source function.

The occupation numbers were determined from the rate equations. For level i we have

$$\begin{aligned} 0 \;=\; & \sum_{k \neq i} n_k \left(A_{ik} + \frac{4\pi}{c} B_{ik} \tilde{J}_{ik} + C_{ik} \right) - \\ & - n_i \sum_{k \neq i} \left(A_{ik} + \frac{4\pi}{c} B_{ki} \tilde{J}_{ki} + C_{ki} \right) \end{aligned} \tag{A6}$$

where the A_{ik} and B_{ik} are the Einstein coefficients for spontaneous and induced radiative transitions, respectively, the C_{ik} are the rate constants for collisional transitions, and the $\tilde{J}_{ik}$ are given by (A2). The energy levels and the Einstein coefficients were derived from the data given by Moruzzi et al. (1995). The C_{ik} were taken from Nagai & Kaifu (1979) and correspond to collisions with H_2 molecules in the rotational ground state ($J = 0$).

A.2. The model molecule

We accounted for 113 rotational levels of the torsional ground state of A-type methanol with $E \leq 180\,\mathrm{cm}^{-1}$, $0 \leq J \leq 14$, and $0 \leq K \leq 6$. Since we wanted to investigate in particular the effects caused by FIR radiation, we additionally accounted in the bulk of our computations for 76 rotational levels in the first torsionally excited state with $E \leq 350\,\mathrm{cm}^{-1}$. Thus, we solved the coupled set of rate equations (A6) for 189 energy levels accounting for 913 spectral lines. - In the context of investigating the suspected new maser lines, we also performed some calculations accounting in the torsionally excited state for all levels with $E \leq 360\ \mathrm{cm}^{-1}$, in total for 198 levels and 979 spectral lines. There were no qualitative changes in the results.

A.3. The background radiation

We performed three sets of calculations with different types of background radiation. In the first set we accounted only for the general 3K background. In the second set we considered the free-free emission from an H II region, writing for the background radiation

$$\begin{aligned} I_{\mathrm{bg}}^{\mathrm{H\,II}} \;=\; & \left[B_\nu(T_{\mathrm{H\,II}}) \left(1 - e^{-\tau_\nu^{\mathrm{H\,II}}} \right) + B_\nu(2.7\mathrm{K}) e^{-\tau_\nu^{\mathrm{H\,II}}} \right] W + \\ & + \; (1 - W) B_\nu(2.7\mathrm{K}) \end{aligned} \tag{A7}$$

Here W is the dilution factor, $T_{\mathrm{H\,II}}$ the kinetic temperature within the H II region (10 000 K) and $\tau_\nu^{\mathrm{H\,II}}$ its optical depth

$$\tau_\nu = g_{\mathrm{ff}} \cdot \frac{1}{\sqrt{T_{\mathrm{H\,II}}}^3} \cdot \frac{EM}{\nu^2} \tag{A8}$$

EM is the emission measure and g_{ff} the gaunt factor. In the third set of calculations we considered as background the IR emission from a layer of warm dust

$$\begin{aligned} I_{bg}^{\mathrm{IR}} \;=\; & \left[B_\nu(T_{\mathrm{dust}}) \left(1 - e^{-\tau_\nu^{\mathrm{IR}}} \right) + B_\nu(2.7\mathrm{K}) e^{-\tau_\nu^{\mathrm{IR}}} \right] W + \\ & + \; (1 - W) B_\nu(2.7\mathrm{K}) \end{aligned} \tag{A9}$$

Here T_{dust} is the dust temperature and τ_ν^{IR} the optical depth of the dust layer. We approximated the frequency dependence of τ_ν^{IR} by

$$\tau_\nu^{IR} = \tau_{30\mu} \left(\frac{\nu}{10^{13}\mathrm{Hz}} \right)^{1.5} \tag{A10}$$

A.4. Range of parameters

With respect to the radiative transfer calculations the maser region is characterized by three free parameters, the kinetic temperature T_{kin}, the hydrogen density $n_{\mathrm{H_2}}$, and the ratio $\nu \cdot N(\mathrm{CH_3OH})/\Delta\nu$, $N(\mathrm{CH_3OH})$ being the column density of the methanol molecules and $^{\Delta\nu}/_{\nu}$ the dimensionless line width. We performed calculations for $T_{kin} = 20, 50$ and 100 K. We varied $n_{\mathrm{H_2}}$ from 10^2 to 10^{12} cm^{-3}. Normalized to $\left(^{\Delta\nu}/_{\nu}\right) = 10^{-5}$ the column density was varied from 10^1 to 10^{20} cm^{-2}. The H II region was characterized by the temperature $T_{\mathrm{H\,II}} = 10\,000\,\mathrm{K}$, the dilution factor $W = 0.5$, and an emission measure of $10^8 \mathrm{pc\,cm}^{-6}$. In the case of IR background radiation we considered dust temperatures $T_{\mathrm{dust}} = 30, 50,$ and 80 K, a dilution factor $W = 0.5$ and an optical depth $\tau_{30\mu\mathrm{m}} = 0.5$.

References

Chandra S., Kegel W.H., Albrecht M.A., Varshalovich D.A., 1984, A&A 140, 295

Cragg D., Johns K., Godfrey P., Brown R., 1992, MNRAS 259, 203

Kegel W.H., 1979, A&AS 38, 131

Menten K., 1991, ApJ 380, L75

Moruzzi G., Winnewisser B., Winnewisser M., Mukhopadhyay I., Strumia F., 1995, Microwave, Infrared and Laser Transitions of Methanol. CRC Press

Nagai T., Kaifu N., 1979, A&AS 31, 317

Ott M., Witzel A., Quirrenbach A., et al., 1994, A&A 284, 331

Piehler G., Kegel W.H., 1989, A&A 214, 339

Slysh V., Kalenskii S., Val'tts I., 1993, ApJ 413, L133

Sobolev A., Cragg D., Godfrey P., 1997, A&A 324, 211